PCCP

Accepted Manuscript

ROYAL SOCIETY OF CHEMISTRY

www.rsc.org/pccp

PCCP

RSCPublishing

ARTICLE

Complex Non-monotonic Thermal Response of Volumetric Space of Simple Liquids

Cite this: DOI: 10.1039/x0xx00000x

M. Chorążewski,[a,#] A. Grzybowski[b,c,*] and M. Paluch[b,c]

Received 00th January 2012,
Accepted 00th January 2012

DOI: 10.1039/x0xx00000x

www.rsc.org/

In this paper, an intricate effect of the isothermal compression of simple liquids on their volumetric response is reported for α,ω-halogenoalkanes as examples. We apply an accurate experimental technique, which is the scanning transitiometry, to directly measure isobaric thermal volume expansivities α_p of the liquids in a wide density range. To thoroughly analyze the observed intersection of the experimental isothermal pressure dependences of α_p, we develop a class of equations of state derived in the density scaling regime for molecular dynamics, finding successful temperature parameterizations of an isothermal equation of state (EOS) intrinsically adapted to describe volumetric data in an extremely wide density range. The EOS based analyses of the scanning transitiomery data as a function of temperature T and pressure p undoubtedly show that the previously considered crossing point of the isothermal dependences $\alpha_p(p)$ is in general represented by a non-linear and non-monotonic curve in the (T-p) phase diagram.

1 Introduction

The knowledge of the thermophysical properties of liquids under elevated pressure is of high interest on account of their wide usage in science and chemical industrial processes. Thermodynamic properties of liquids are crucial for designing chemical processes as well as for verifying modern equations of state. From many physicochemical properties of fluids, the isobaric coefficient of thermal expansion, $\alpha_p \equiv V^{-1}\left(\partial V/\partial T\right)_p$, stands out. The isobaric expansivity α_p can be expressed by the second mix derivative of the Gibbs potential with respect to pressure p and temperature T, $\partial^2 G/\partial p \partial T = \partial^2 G/\partial T \partial p = \left(\partial V/\partial T\right)_p = -\left(\partial S/\partial p\right)_T = -T^{-1}\left(\partial Q/\partial p\right)_T$. The Maxwell relation between entropy and volume changes shows that the heat absorbed per unit volume in a pressure reduction depends on the same derivative as the work done per unit volume in a thermal expansion.

Accurate liquid thermal expansivities, α_p, over large ranges of pressure and temperature are needed in many engineering problems where changes in dimension or density due to temperature are expected, such as process simulations, equipment and pipe design. For example, the thermal expansion coefficient is a property of great interest, since it is involved in the oil and automotive industry,[1] where temperatures of about 200°C and pressures of about 200 MPa are routinely encountered. For instance, a highly efficient and properly constructed fuel injection system is one of the most important key components, which determine emissions and fuel consumption. Injector geometry, nozzle designs, fuel pump and injection pressure are keys to the ideal injection process condition. In the modern generation of common rail direct diesel fuel injection system, the fuel pressure can reach up to 200 MPa. It is important therefore to be able to measure thermophysical properties of liquid fuels under such extreme conditions for tests and further development in the industry branch. As an example, NADIA-bio (*New Advanced Diagnosis for Diesel Injection Analysis and bio fuels*) French automotive federative project around hydraulics of common rail systems has improved 1D simulation of fuel circuits and developed a completely new injection test bench operating with actual fuels with known thermophysical properties at different temperature levels.[2] The thermal expansion coefficient over a large range of pressures and temperatures is also one of the important real fuel physicochemical properties introduced to AMESim numerical tools in order to solve the continuity equation and the energy equation.

In practice, α_p is not usually measured directly. Several techniques are available to calculate isobaric thermal expansivity of liquids under elevated pressure. Among the nonthermal techniques, density measurements[3,4,5,6,7,8] or correlations,[9,10] pVT - volumetric technique,[11] and sound speed measurements[12] are the most important. The experimental significance of the mentioned Maxwell relations comes mainly from the fact that the thermomechanical coefficient $\left(\partial V/\partial T\right)_p$ can be determined directly from calorimetric measurements of the heat Q developed by variations of pressure, performed under isothermal conditions.[13] The respective techniques are known as piezothermal technique,[14,15] pressure-controlled calorimetry,[13,16,17,18,19] and pressure perturbation calorimetry.[20,21]

Scanning transitiometry,[22,23] actually the most direct technique for determining thermal expansion of liquids, is a further development of pVT controlled scanning calorimetry,[13] which was devoted to measurements of heat effects associated with variations of the state variables. The simultaneous recording of both the heat flow and volume changes resulting from a given pressure change under isothermal conditions leads to the simultaneous determination of thermal and mechanical contributions to the thermodynamic potential change caused by the perturbations. The opportunity for isothermal pressure scanning direct measurement of thermal expansion, which is the second order derivative of the thermodynamic potential, is the unique property of scanning transitiometry.[23]

The transitiometer, BGR TECH, Warsaw, Poland has already been described previously.[24] More details of the calibration procedure and determined thermal expansivities of liquid toluene critically analyzed against existing literature data can be found in a previous paper.[24] The relative uncertainty for the determination of thermal expansivities was found to be of 2%, while the repeatability of the present measurements is estimated to be ±0.5%.

The direct measurements of isobaric thermal expansivity, the second derivative of the thermodynamic potential, over large pressure and temperature ranges permit accurate calculations (usually by integration) of related thermodynamic properties and key thermophysical properties over extended temperature and pressure ranges. The isobaric coefficient of thermal expansion is a quite sensitive to subtle changes in density, and hence its analysis provides more information about molecular interactions in the liquid state and consitutes a useful basis for understanding the nature of liquid.[25,26,27] A general observation of the pressure dependences of the isobaric thermal expansivities for many liquids shows that the dependences $\alpha_p(p)$ decrease with increasing pressure at constant temperature and the isotherms intersect at high pressures, i.e., exhibit a unique crossing point at a single value of pressure,[1,3,5,7,12,15,24-27] at which $\left(\partial\alpha_p/\partial T\right)_p = 0$. Randzio and Dieters[28,29] concluded that the existence of the unique intersection point is a key feature for examining and testing equations of state. Very recent studies mainly based on theoretical predictions[25] or focused on specific materials, which are ionic liquids,[30] have strongly suggested that the intersection point should be rather considered as an intersection curve which is in general nonlinear in the pressure-temperature space. Although such a behavior has been also reported for simple liquids,[27] it has been suggested after exploiting a phenomenological equation of state formulated specially to describe the intersection of the isothermal dependences $\alpha_p(p)$.

In this paper, we show that the complex non-monotonic behavior of thermal expansivity measured by means of the scanning transitiometry is observed even for simple liquids such as 1,3-dichloropropane (1,3-diClC3) and 1,5-dichloropentane (1,5-diClC5). To thoroughly investigate this phenomenon, we develop a class of equations of state very recently derived in the density scaling regime by some of us with no preliminary expectations that the intersection of the isotherms $\alpha_p(p)$ will occur, but focusing only on the description of volumetric properties of simple liquids, the total instantaneous virial W and the total instantaneous potential energy U of which are suggested to obey a strong isochoric linear correlation.

2 Results and discussion

2.1 Equations of State for Simple Liquids

Equations of state are key elements in the study of the thermodynamic behavior of physical systems. They describe the relationships that exist between relevant extensive and intensive parameters for a given system, and thus they are useful tools for prediction of thermodynamic properties of substances. To investigate pressure dependences of the isobaric volume expansivities determined from isothermal measurements carried out by means of the scanning transitiometry, we have exploited a class of interrelated equations of state recently derived[31,32,33,34,35,36] in two ways: (i) using a modification of the definition of the isothermal bulk modulus and (ii) considering an effective intermolecular potential that has been suggested to be responsible for so-called "density scaling" of molecular dynamics. The density scaling idea has been initiated by studying molecular dynamics of glass-forming liquids in high pressure conditions.[37,38] Phenomenological analyses of experimental data of supercooled liquids, mainly van der Waals liquids and polymer melts, have shown that dynamic quantities such as structural relaxation times τ or viscosities η determined from isobaric and isothermal measurements at various pressures can be plotted onto one master curve as a function of a single variable $\Gamma = \rho^{\gamma}/T$, where T and ρ denote temperature and density, respectively, and γ is a material constant independent of thermodynamic conditions. It has been argued[39,40,41,42,43,44,45,46] that the scaling exponent γ is straightforwardly related to the exponent of the dominant repulsive part of an effective intermolecular potential $U_{eff}(r) = 4\varepsilon(\sigma/r)^{m_{IPL}} - A_t$, which is a proper short-range approximation of the generalized Lennard-Jones potential, $U_{LJ}(r) = 4\varepsilon(\sigma/r)^m - 4\varepsilon(\sigma/r)^n$. The theoretical and simulation investigations have shown that $m_{IPL} > m$ and A_t is a small constant or linear attractive background. What is more, it has been found that the scaling exponent $\gamma \cong m_{IPL}/3$.

This simple idea has strongly encouraged to derive an equation of state (EOS) from the same theoretical grounds that have been suggested to explain the density scaling of molecular dynamics. Such an EOS has been first formulated in an isothermal version[31] on the assumption of the effective short-range potential U_{eff}. It has been shown[33] that one can also arrive at the isothermal EOS based on the definition of the isothermal configurational bulk modulus, $B_T^{conf} = \left(\partial \ln\rho/\partial p^{conf}\right)_T$, where p^{conf} is the configurational pressure defined by the equation, $p^{conf} = p - RTM^{-1}\upsilon^{-1}$ with the pressure p, the gas constant R, and the specific volume $\upsilon = \rho^{-1}$. In this way, the applicability range of the EOS has been established to be limited to the linear pressure dependence of the isothermal configurational bulk modulus. In addition, an alternative isothermal EOS has been formulated[33] from the definition of the bulk modulus, $B_T = \left(\partial \ln\rho/\partial p\right)_T$, the applicability range of which is limited to the linear pressure dependence of the isothermal bulk modulus (eqn 2). Subsequently, both the isothermal EOSs have been successfully parameterized[34] by two temperature functions at a reference pressure p_0 such as a polynomial temperature function of volume and an exponential temperature function of isothermal bulk modulus. In this paper, we employ the following EOS originally reported as eqn (9) in Ref. 34,

$$\upsilon(T,p) = \upsilon(T,p_0)\left[1 + \frac{\gamma}{B_T(p_0)}\left(p - p_0\right)\right]^{-1/\gamma} \tag{1a}$$

$$\upsilon(T,p_0) = \sum_{l=0}^{k} A_l (T - T_0)^l \tag{1b}$$

$$B_T(p_0) = b_0 \exp(-b_2(T - T_0)) \tag{1c}$$

where $b_0 = B_{T_0}(p_0)$, $b_2 = b_2(p_0) = -\partial \ln B_T(p_0,T)/\partial T\big|_{T=T_0}$, $A_0 = \upsilon(T_0,p_0)$, and $A_l = (1/l!)\partial^l \upsilon(p_0,T)/\partial T^l\big|_{T=T_0}$ for l=1,2,.. .

The isothermal and parameterized EOSs based on both the definitions of B_T and B_T^{conf} have been successfully tested by using pVT measurement data for various liquids from different material groups such as van der Waals liquids, polymer melts, aprotic and protic ionic liquids, and associated liquids.[31-34,47,48,49,50,51,52,53,54,55,56] The analyses based on the mentioned various experimental pVT data as well as molecular dynamics (MD) simulation studies[35] have confirmed that each of the EOSs yields numerically equivalent values of the scaling exponent γ, which can be for instance found[32,55] as a slope of the linear dependence of B_T on pressure at a constant temperature *T*,

$$B_T(p) = B_T(p_0) + \gamma(p - p_0) \tag{2}$$

where p_0 is a reference pressure. It means that the class of equations of state is well-interpreted in terms of the effective short-range intermolecular potential U_{eff}, the dominant repulsive term of which is proportional to $r^{-3\gamma}$.

The limitation of eqn (1a) given by eqn (2) has been originally argued[31-35] by a low compressibility of investigated glass formers. Nevertheless, eqn (2) can be also valid in another compressibility range depending only on its width. Similar comments can be made on the limitations of eqn (1a) given by eqn (1b) and (1c). For instance, it should be noted that eqn (1a) with the parameterizations (eqn (1b) and (1c)) has been until recently used to fit very satisfactorily the pVT experimental data measured within the density range of about 0.15g/cm^3. However, very recent theoretical and simulation investigations suggest that both the recipe for the density scaling of molecular dynamics and the corresponding EOS should be extended if the system density considerably varies.

The theory of isomorphs,[57,58,59] which provides an advanced description of the general density scaling of molecular dynamics, substantiates the previous suggestions[40] that the general density scaling law is given by the equation, $X(\rho,T) = f(h(\rho)/T)$, where e.g. $X = \tau,\eta$, and the scaling exponent γ is defined[60] by a logarithmic derivative of the density function $h(\rho)$, $\gamma = d\ln h/d\ln\rho$, which can be in general a density function $\gamma(\rho)$. The generalization about the density scaling shows that the typical power law density scaling with a material constant γ is obeyed if the function, $h(\rho) = \rho^\gamma$. However, the theory of isomorphs implies that systems characterized even by such a simple intermolecular potential like the Lennard-Jones (LJ) potential requires the general density scaling law if we consider a sufficiently wide density range. This prediction has been confirmed by means of MD simulations of the Kob-Andersen binary Lennard-Jones (KABLJ) mixtures.[61] The structural relaxation times obtained in the KABLJ model can be scaled with a constant value of γ to a good approximation in the density range between 1.2 to 1.6 in LJ units, especially if we use the reduced units suggested by Dyre's group to ensure the molecular dynamics to be isomorph invariant. However, the extension of the density range up to 2.0 in LJ units leads to the scaling exponent γ which varies with density changing. Very recently, eqn (1) and its counterpart based on B_T^{conf} have been developed[36] to comply with the general density scaling law. These EOSs have been successfully used to describe pVT data collected in the density range between 1.2 to 2.0 in LJ units for the KABLJ model. What is more, the density functions, $h(\rho)$ and $\gamma(\rho)$, parameterized by fitting the pVT data in the KABLJ model to these EOSs, have enabled to scale very well the structural relaxation times in the KABLJ model. Thus, these new EOSs are proper generalizations about eqn (1) and its counterpart based on B_T^{conf}, because their precursors are able to provide a constant scaling exponent by fitting pVT data in the KABLJ model, which leads to the typical power law density scaling of structural relaxation times in the KABLJ model.

In context of the mentioned theoretical and simulation studies, it is very interesting to verify the effect of density range on the applicability of eqn (1) in the case of the liquid α,ω-halogenoalkanes examined herein. To do that we need to parameterize the new EOSs, which have been derived in Ref. 36 as isothermal equations. We focus herein on eqn (14) in Ref. 36 with the density functions, $h(\rho)$ and $\gamma(\rho)$, given respectively by eqn (21) and (22) in Ref. 36. We assume the same parameterizations as those used in eqn (1), because the temperature-pressure range of the scanning transitiometry experiment suggests that the temperature functions given by eqn (1b) and (1c) should be sufficient to properly describe the volume and the isothermal bulk modulus at a reference pressure. Thus, the following EOS is employed in this paper as the extension of eqn (1) to the thermodynamic region within which the general density scaling law is valid,

$$p = p_0 + \frac{B_T(p_0)}{\gamma(\rho_0)}\left(\frac{h(\rho)}{h(\rho_0)} - 1\right) \tag{3a}$$

$$h(\rho) = \exp\left(C_1 \ln\rho + C_2 \ln^2\rho\right) \tag{3b}$$

$$\gamma(\rho) = C_1 + 2C_2 \ln\rho \tag{3c}$$

$$\rho_0 = \upsilon^{-1}(T, p_0) = \left(\sum_{l=0}^{k} A_l (T - T_0)^l\right)^{-1} \tag{3d}$$

$$B_T(p_0) = b_0 \exp(-b_2(T - T_0)) \tag{3e}$$

The general EOS given by eqn (3) can be reduced to eqn (1) by taking $C_2 = 0$. Then, $C_1 = \gamma$, which is a constant scaling exponent, and $h(\rho) = \rho^\gamma$. In contrast to eqn (2), the applicability range of eqn (3) is defined by in general a nonlinear pressure dependence of the isothermal bulk modulus (eqn (18) in Ref. 36), which involves the density dependent scaling exponent $\gamma(\rho)$,

$$B_T(p) = \frac{\gamma(\rho)}{\gamma(\rho_0)}\left[B_T(p_0) + \gamma(\rho_0)(p - p_0)\right] \tag{4}$$

The above nonlinear pressure dependence of the isothermal bulk modulus reduces to the linear pressure dependence given by eqn (2) if we apply eqn (3c) with $C_2 = 0$ to eqn (4).

We have analyzed the isobaric volume expansivity data (collected in Table 1 in Electronic Supplementary Information (ESI)†) determined from isothermal scanning transitiometry experiments in terms of eqn (1) and (3), which lead respectively to the following formulae for the volume expansivity via the definition of the isobaric volume expansivity,

$$\alpha_p(T,p) = \alpha_p(T,p_0) + \frac{p - p_0}{B_T(p_0) + \gamma(p - p_0)}\left(\frac{\partial \ln B_T(p_0)}{\partial T}\right)_p \tag{5}$$

$$\alpha_p(T,p) = \frac{\gamma(\rho_0)}{\gamma(\rho)}\left[\alpha_p(T,p_0) + \frac{p - p_0}{B_T(p_0) + \gamma(\rho_0)(p - p_0)}\left(\frac{\partial}{\partial T}\ln\left(\frac{B_T(p_0)}{\gamma(\rho_0)}\right)\right)_p\right] \tag{6}$$

where $B_T(p_0)$ is parameterized in the same way given by eqn (1c) and (3e), and then $\partial \ln B_T(p_0)/\partial T = -b_2$, which is a parameter independent of thermodynamic conditions. The function $\gamma(\rho)$ is defined by eqn (3c), and eqn (3d) parameterizes the density $\rho_0 = \upsilon^{-1}(T, p_0)$ at a reference pressure p_0. Thus, the expansivity at a reference pressure p_0 can be calculated via the derivative, $\alpha_p(T,p_0) = -\partial \ln\rho(T,p_0)/\partial T$. Based on eqn (3c), one can determine the derivative $\partial \ln\gamma(\rho_0)/\partial T = -2C_2\alpha_p(T,p_0)/\gamma(\rho_0)$. Then, one can see that eqn (6) derived from eqn (23) in Ref. 36 reduces to eqn (5) if $C_2 = 0$, because it also implies $\gamma(\rho) = \gamma(\rho_0) = const$.

2.2 The EOS based analysis of scanning transitiometry data

To fit the isobaric volume expansivity as a temperature-pressure function $\alpha_p(T,p)$, we have assumed that the reference state (T_0,p_0) in case of both the EOSs (eqn (1) and (3)) is the melting point at ambient pressure, which is equal to T_0=174.15K and T_0=201.15K for 1,3-diClC3 and 1,5-diClC5, respectively. Such a choice of the reference state is reasonable, because the sought after values of the fitting parameters in both the EOSs are dedicated to the liquid state of the examined α,ω-dichloroalkanes. We have also tested results of the fitting of $\alpha_p(T,p)$ to eqn (5) and (6) on the assumption of another reference state, which is defined at the lowest temperature (T=273.15K) of the experimental isotherm at ambient pressure. We have found that the quality of the fits to eqn (5) and (6) does not depend on the chosen reference states although they are considerably different. Nevertheless, we have established that the complex non-trivial temperature-pressure dependence of α_p requires a cubic temperature parameterization of the volume at the reference pressure in case of both the EOSs (eqn (1b) and (3d) with k=3). Moreover, we have obtained that eqn (5) based on the EOS given by eqn (1) is able to describe successfully the pressure dependences of α_p determined at constant temperatures that range from T=273.15K to T=373.15K, where the adjusted coefficients of determination for the nonlinear regressions, adj-R^2 ≈ 0.9966 and adj-R^2 ≈ 0.9913 for 1,3-diClC3 and 1,5-diClC5, respectively. The values of all the fitting parameters of eqn (1) for both the investigated α,ω-dichloroalkanes are collected in Table 2 in ESI† and the corresponding dashed fitting curves are presented in the insets in Figs. 1(a) and 2(a). Although our attempts at applying eqn (1) to all the set of isotherms of the isobaric volume expansivities determined for each examined α,ω-dichloroalkane at temperatures that range from T=273.15K to T=423.15K have been completed quite satisfactorily, we have observed that some fitted curves deviate from the dependences $\alpha_p(T,p)$ determined from the scanning transitiometry experiments in the highest experimental pressure limit, which has not been shown herein. Therefore, we have tested whether the discrepancy can be removed by applying eqn (6) based on the EOS given by eqn (3) to fit the dependences $\alpha_p(T,p)$ in all the temperature-pressure range explored experimentally. As a result, we have obtained that eqn (6) based on the EOS given by eqn (3) yields the best fits of all the examined dependences of $\alpha_p(T,p)$ for both the liquid α,ω-dichloroalkanes. The values of the fitting parameters of eqn (3) are collected in Table 3 in ESI† and the corresponding fitted curves are shown in Figs. 1(a) and 2(a). The obtained adjusted coefficients of determination for the nonlinear regressions, adj-R^2 ≈ 0.9969 and adj-R^2 ≈ 0.9921 for 1,3-diClC3 and 1,5-diClC5, respectively. One can assess the qualities of the fits as quite good, taking into consideration the complex set of experimental data collected and analyzed as a temperature-pressure function of α_p.

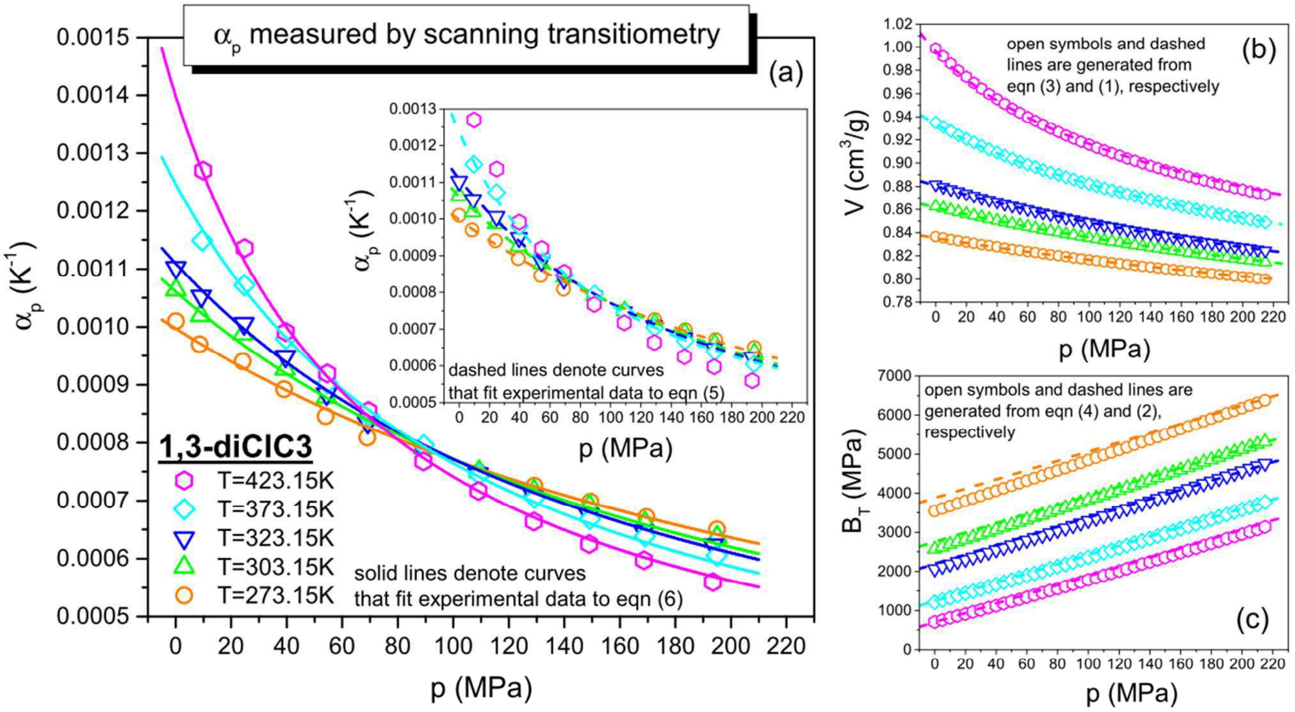

Fig. 1. (a) Plot of the pressure dependence of the isobaric thermal expansivity of 1,3-diClC3 measured by scanning transitiometry in isothermal conditions. The solid lines denote curves that fit experimental data to eqn (6). The inset shows the same experimental data fitted to eqn (5) in the temperature range from 273.15K to 373.15K. (b) Plot of the pressure dependences of specific volume at experimental temperatures. Open symbols and dashed lines are generated respectively from eqn (3) and (1) using values of their parameters obtained from fits presented in panel (a) and collected in Tables 2 and 3 in ESI†. (c) The corresponding pressure dependences of the isothermal bulk modulus generated from eqn (4) and (2), open symbols and dashed lines, respectively.

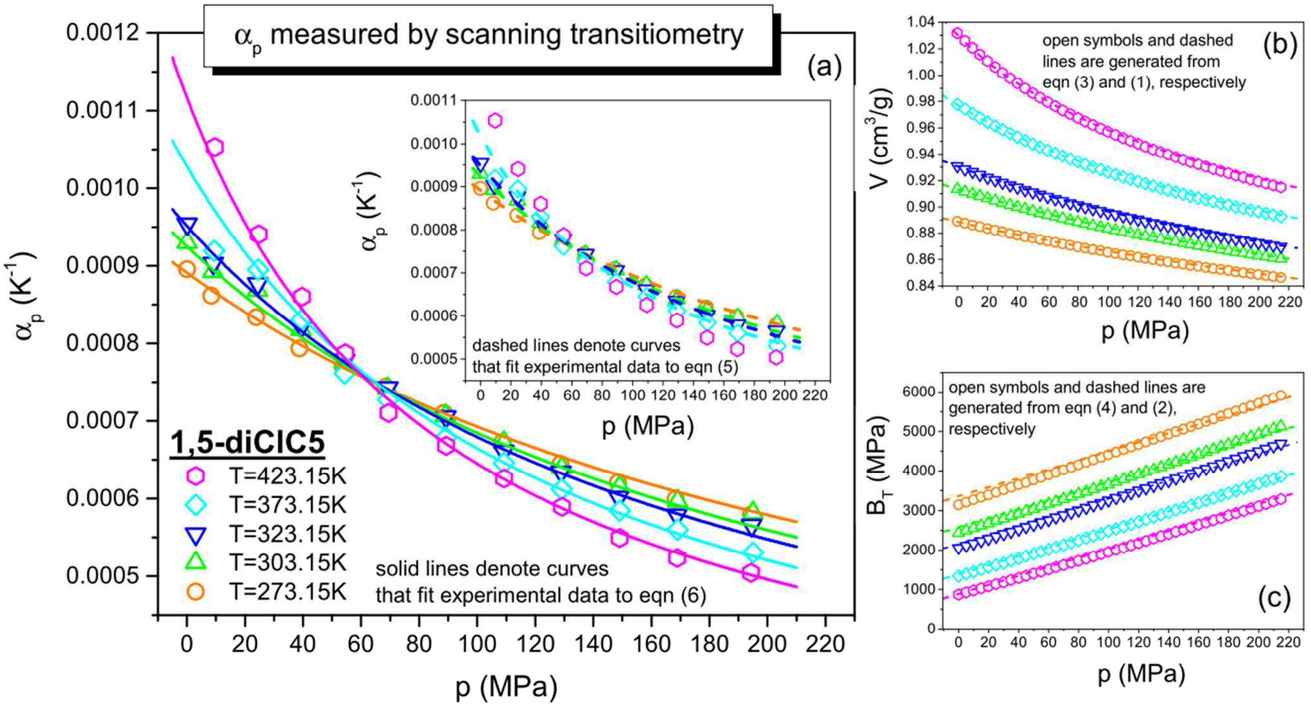

Fig. 2 (a) Plot of the pressure dependence of the isobaric thermal expansivity of 1,5-diClC5 measured by scanning transitiometry in isothermal conditions. The solid lines denote curves that fit experimental data to eqn (6). The inset shows the same experimental data fitted to eqn (5) in the temperature range from 273.15K to 373.15K. (b) Plot of the pressure dependences of specific volume at experimental temperatures. Open symbols and dashed lines are generated respectively from eqn (3) and (1) using values of their parameters obtained from fits presented in panel (a) and collected in Tables 2 and 3 in ESI†. (c) The corresponding pressure dependences of the isothermal bulk modulus generated from eqn. (4) and (2), open symbols and dashed lines, respectively.

The fitting results obtained in terms of eqn (1) and (3) can be rationalized by comparison with the above discussed results of MD simulations in the KABLJ model, for which the increase of 100% in the density range (i.e., from 1.2-1.6 in LJ units to 1.2-2.0 LJ units) disabled to scale structural relaxation times using a constant value of the scaling exponent γ.[36,61] In the wide density range, it has been shown that eqn (3a) instead of eqn (1a) enables to find the scaling exponent that depends on density and leads to the density scaling of structural relaxation times in the KABLJ model in the density range from 1.2 to 2.0 LJ units. As mentioned, eqn (1) has been until recently applied to describe pVT data measured typically in the density range of about 0.15g/cm^3. However, the experimental isothermal data of $\alpha_p(T,p)$ for both the examined α,ω-dichloroalkanes correspond to the density range of about 0.15g/cm^3 for isotherms measured between 273.15K and 373.15K. The increase in the explored temperature range by 50K, which results from the extension of the set of isothermal data by the isotherm $\alpha_p(T,p)$ measured at T=423.15K, causes the increase of about 50% in density of each studied system (see Figs. 1(b) and 2(b)). Thus, although the transitiometry measurements of $\alpha_p(T,p)$ are carried out in the pressure range of 200MPa, which is a typical measurement pVT range, the wide measurement temperature range results in a quite wide density range in the case of examined substances. Consequently, the experimental data $\alpha_p(T,p)$ are better described by eqn (3) than by eqn (1), because eqn (3) is intrinsically adapted[36] to volumetric data measured in the wide density ranges 1.00g/cm^3 < ρ < 1.25 g/cm^3 and 0.97g/cm^3 < ρ < 1.18 g/cm^3 for 1,3-diClC3 and 1,5-diClC5, respectively. Nevertheless, the fitting curves obtained from eqn (1) for the specific volume only slightly deviate (see Figs 1(b) and 2(b)) from those determined from eqn (3). Similarly, the pressure dependences of the isothermal bulk modulus generated from eqn (2) and (4), which are based on the EOSs given respectively by eqn (1) and (3), are quite close to each other to a good approximation (see Figs. 1(c) and 2(c)). However, the differences between the dependences $B_T(p)$ generated from eqn (2) and (4) are larger at the lowest temperatures in contrast to those observed form the specific volumes generated from eqn (1) and (3). This apparently surprising result is a consequence of the different contribution of the intermolecular potential to the specific volume and the isothermal bulk modulus, which can be deduced from the EOSs given by eqn (1) and (3), and their implications (eqn (2) and (4)), which describe the dependences $B_T(p)$. One can see that the term related to the intermolecular potential in the EOSs is the reduced scaling function, $h(\rho)/h(\rho_0)$, however, the derivative definition, $B_T = (\partial \ln\rho/\partial p)_T$, causes that the reduced scaling exponent $\gamma(\rho)/\gamma(\rho_0)$ mainly reflects the contribution given by the intermolecular potential to the dependence $B_T(p)$. We have verified that the quotients $h(\rho)/h(\rho_0)$ calculated in terms of eqn (1) and (3), where $h(\rho)=\rho^\gamma$ for eqn (1), are very close numbers, which begin to deviate from each other only at low densities. On the other hand, the quotients $\gamma(\rho)/\gamma(\rho_0)$ in eqn (3) is in general different from those valid for eqn (1), because $\gamma(\rho)/\gamma(\rho_0)=1$ in eqn (1). For this reason, the largest differences in the dependences $B_T(p)$ generated from eqn (2) and (4) are observed at the lowest temperatures that correspond to the highest densities at which the differences in the values of the effective short-range potential parameters suggested to be reflected in the function $\gamma(\rho)$ exert the strongest effect on the volumetric properties.

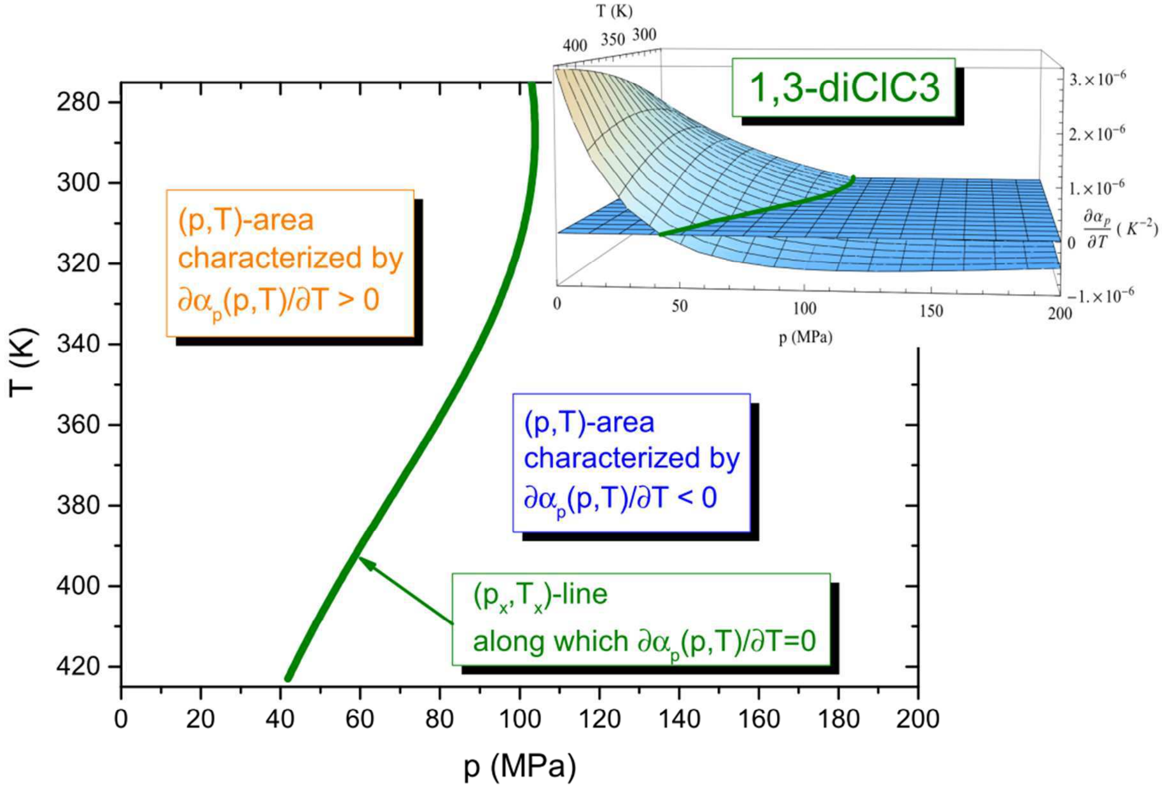

Fig. 3. Plot of the phase diagram for the simple liquid 1,3-diClC3, where the solid line denotes points (p_x,T_x) at which $(\partial\alpha_p(p,T)/\partial T)_p=0$. The solution of the latter equation, which exploits eqn (6), is graphically demonstrated in the inset.

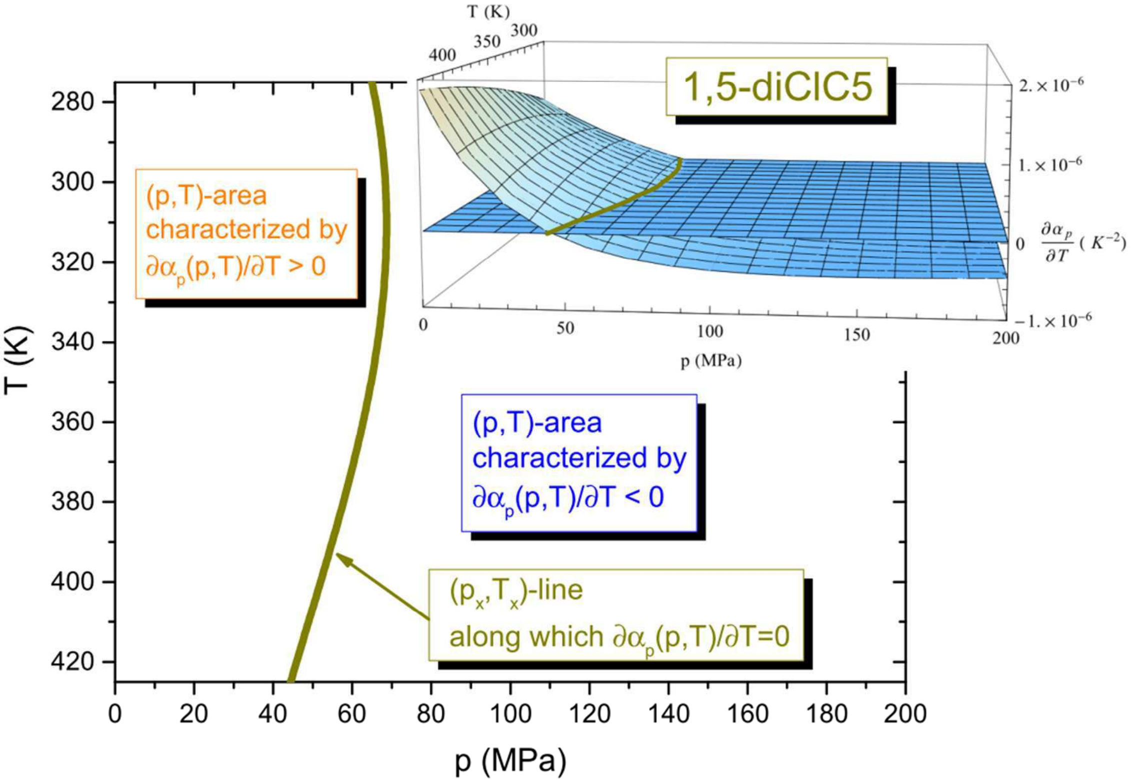

Fig. 4. Plot of the phase diagram for the simple liquid 1,5-diClC5, where the solid line denotes points (p_x,T_x) at which $(\partial\alpha_p(p,T)/\partial T)_p$=0. The solution of the latter equation, which exploits eqn (6), is graphically demonstrated in the inset.

An extremely interesting problem investigated by us using eqn (1) and (3) is the crossing point expected for the isothermal dependences $\alpha_p(p)$. As can be seen in Figs. 1(a) and 2(a), the experimental isothermal dependences $\alpha_p(p)$ cross each other rather within a pressure range than at a pressure of a single value, which can result from measurement uncertainties of α_p or be a consequence of a more complex behavior of the solution of the equation $\left(\partial\alpha_p(T,p)/\partial T\right)_p=0$. It should be noted that the latter solution can be in general a function of temperature and pressure. Using eqn (6) based on eqn (3), we have numerically solved the equation with respect to pressure in isothermal conditions explored every temperature degree within the experimental temperature range (273.15K ≤ T ≤ 423.15K), which is graphically demonstrated in the insets in Figs. 3 and 4. As a result, we have established that the curve determined on condition that $\left(\partial\alpha_p(T,p)/\partial T\right)_p=0$ is neither point nor straight line. For both the tested α,ω-dichloroalkanes (see Figs. 3 and 4), we have found that such a curve is nonlinear and has a non-monotonic character. Then, we have extrapolated (see Fig. 5) the domain of this analysis to vary between the melting temperature and the boiling temperature at ambient pressure (extending the domain to the highest experimental temperature in case of 1,3-diClC3). In this way, we have shown a maximum in the border line $p_x(T_x)$ which separates the (T,p)-areas characterized respectively by negative and positive values of $\left(\partial\alpha_p(T,p)/\partial T\right)_p$ in the phase diagram of both 1,3-diClC3 and 1,5-diClC5.

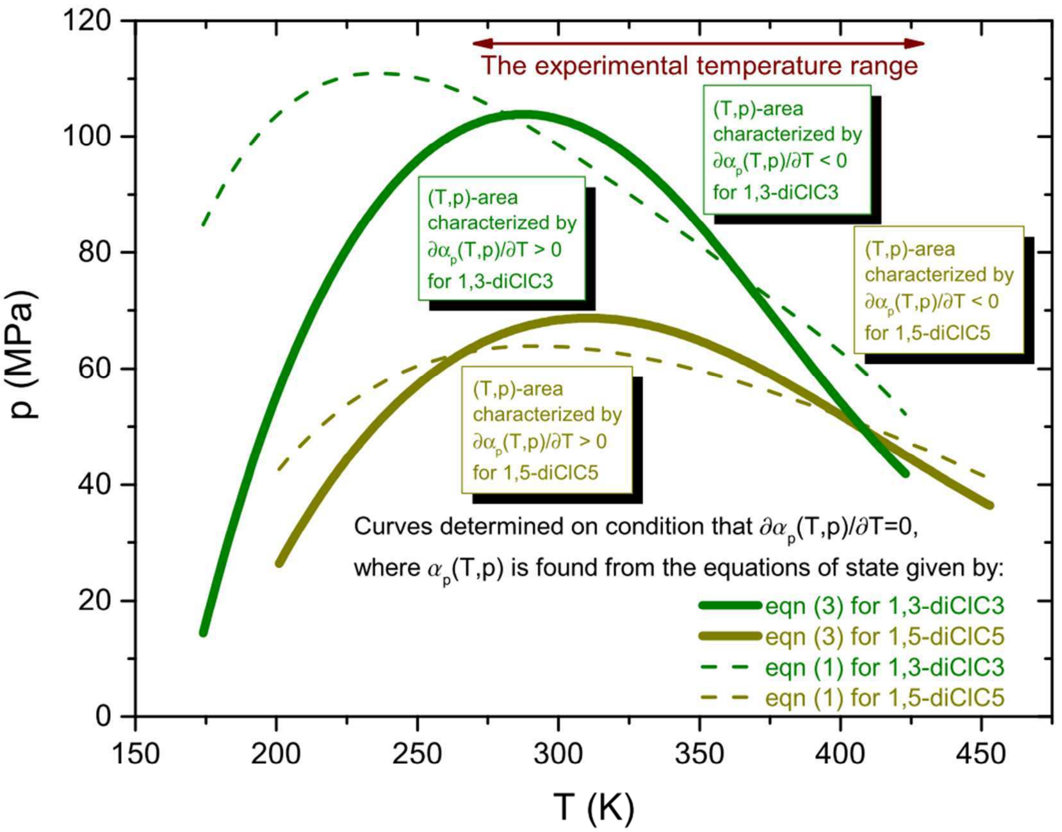

Fig. 5. Plot of the phase diagrams for the simple liquids 1,3-diClC3 and 1,5-diClC5. The solid and dashed lines denote points (p_x,T_x) found on condition that $(\partial\alpha_p(p,T)/\partial T)_p=0$ using eqn (6) and (5), respectively.

In addition, we have followed an analogous procedure to evaluate the border line $p_x(T_x)$ by using eqn (5) based on eqn (1). Consequently, we have obtained qualitatively the same non-monotonic behavior of the border line for both the α,ω-dichloroalkanes as those established from eqn (6) based on eqn (3). In the experimental temperature range, the border line is evaluated from both the EOSs within the different pressure ranges, $40\text{MPa} \lesssim p \lesssim 105\text{MPa}$ and $40\text{MPa} \lesssim p \lesssim 70\text{MPa}$, for 1,3-diClC3 and 1,5-diClC5, respectively, which seem to be related to a proximity effect[62,63] according to which properties of the molecules depend on the distance between the terminal halogen atoms. However, the maxima in $p_x(T_x)$ found from eqn (1) are considerably shifted to lower temperatures and do not match those obtained from eqn (3), especially in the case of 1,3-diClC3. The deviation of the evaluation based on eqn (1) from the solution of the equation $\left(\partial\alpha_p(T,p)/\partial T\right)_p=0$, which exploits eqn (3), has a similar origin to that discussed for the dependences $B_T(p)$. This is because eqn (6) similarly to eqn (4) involves the quotient $\gamma(\rho)/\gamma(\rho_0)$, which distinguishes the representation of the dependence $\alpha_p(T,p)$ from that given by eqn (5) based on eqn (1).

3 Summary and conclusions

To sum up, our scanning transitiometry study of thermal expansivity of α,ω-dichloroalkanes in the typical pressure range (0.1MPa ≤ p ≤ 200MPa) shows that there is a non-monotonic border line in the phase diagram of each examined simple liquid, which divides the phase diagram into two areas characterized by opposite thermal volume expansivities. To investigate this intriguing behavior, we have developed and successfully tested the equation of state (eqn (3)), which has been intrinsically adapted[36] to describe an extremely wide density range. This EOS as well as its precursor (eqn (1)) provide useful relations (eqn (3b) and (3c) and their counterparts for eqn (1)) between the macroscopic volumetric properties and the effective intermolecular potential suggested to be relevant to molecular dynamics of simple liquids, which is expected to comply with the strong isochoric linear correlation between the system virial and the system potential energy. By applying the class of novel equations of state to solve the equation $\left(\partial\alpha_p(T,p)/\partial T\right)_p=0$, we have confirmed the existence of the invariant temperature-pressure function α_p along the non-monotonic (p_x,T_x)-line for the examined dichloroalkanes. Our findings strongly suggest that the non-monotonic behavior aspire to be a general property of various liquids instead of the previously considered crossing point of the isothermal dependences $\alpha_p(p)$.

Acknowledgements

A.G. and M.P. are grateful for the financial support obtained within the program MAESTRO 2 (the decision no. DEC-2012/04/A/ST3/00337) from the Polish National Science Center.

Notes

[a] Institute of Chemistry, University of Silesia, Szkolna 9, 40-006 Katowice, Poland.

[b] Institute of Physics, University of Silesia, Uniwersytecka 4, 40-007 Katowice, Poland.

[c] Silesian Center for Education and Interdisciplinary Research, 75 Pułku Piechoty 1A, 41-500 Chorzów, Poland.

[*] Corresponding author's email: andrzej.grzybowski@us.edu.pl.

[#] Corresponding author's email: miroslaw.chorazewski@us.edu.pl.

† Electronic Supplementary Information (ESI) available: The ESI includes experimental isothermal data of the isobaric thermal expansivities α_p for 1,3-diClC3 and 1,5-diClC5 measured by the scanning trasitiometry as well as values of the parameters of their fits to the temperature-pressure functions $\alpha_p(T,p)$ given by eqn (5) and (6) that follow respectively from the equations of state given by eqn (1) and (3). See DOI: 10.1039/b000000x/

References

1 M. Chorążewski, F. Dergal, T. Sawaya, I. Mokbel, J-P.E. Grolier and J. Jose, *Fuel*, 2013, **105**, 440.
2 J.B. Blaisot, J-L. Daridon, C. Garsi, P. Gastaldi, J-P. Grolier, S. Honnet, B. Loyer, P. Manuelli, L. Mees, I. Mokbel, B. Reveille, R. Saliba, M. Zellat, *Nadia_bio: New Advanced Diagnosis for Diesel Injection Analysis and bio fuels. A federative project around hydraulics of CR systems.* International Conference: Diesel Powertrain, Innovative Technologies for Future Emissions Targets, Rouen, France – INSA, June 5 - 6, 2012.
3 J. L. Valencia, D. González-Salgado, J. Troncoso, J. Peleteiro, E. Carballo and L. Romaní, *J. Chem. Eng. Data*, 2009, **54**, 904.
4 J. J. Segovia, O. Fandiño, E. R. López, L. Lugo, M. Carmen Martín and J. Fernández, *J. Chem. Thermodyn.*, 2009, **41**, 632.
5 C. A. Cerdeiriña, C.A. Tovar, D. González-Salgado, E. Carballo and L. Romani, *Phys. Chem. Chem. Phys.* 2001, **3**, 5230.
6 M. J. P. Comuñas, J.–P. Bazile, A. Baylaucq and Ch. Boned, *J. Chem. Eng. Data*, 2008, **53**, 986.
7 J. Troncoso, D. Bessières, C. A. Cerdeiriña, E. Carballo and L. Romani, *Fluid Phase Equilib.*, 2003, **208**, 141.
8 Ch. Boned, A. Baylaucq and J.-P. Bazile, *Fluid Phase Equilib.*, 2008, **270**, 69.
9 I. Cibulka and T. Takagi, *J. Chem. Eng. Data*, 1999, **44**, 411.
10 Lemmon, E.W., Span, R. Short Fundamental Equations of State for 20 Industrial Fluids. *J. Chem. Eng. Data* **51**, 785-850 (2006).
11 H. Machida, Y. Sato and R. L. Smith Jr., *Fluid Phase Equilib.*, 2008, **264**, 147.
12 M. Chorążewski and M. Skrzypek, *Int. J. Thermophys.*, 2010, **31**, 26.
13 S. L. Randzio, *Thermochim. Acta*, 1985, **89**, 215.
14 Ph. Pruzan, L. Ter Minassian, P. Figuiere and H. Szwarc, *Rev. Sci. Instrum.*, 1976, **47**, 66.
15 L. Ter Minassian and Ph. Pruzan, *J. Chem. Thermodyn.*, 1977, **9**, 375.
16 S. L. Randzio, *J. Phys. E: Sci. Instrum.*, 1983, **16**, 691.
17 S. L. Randzio, *J. Phys. E: Sci. Instrum.*, 1984, **17**, 1058.
18 S. L. Randzio, J-P. E. Grolier and J. R. Quint, *Rev. Sci. Instrum.*, 1994, **65**, 960.
19 P. Navia, J. Troncoso and L., Romaní, *J. Chem. Thermodyn.*, 2008, **40**, 1607.
20 P. Kujawa and F. M. Winnik, *Macromolecules*, 2001, **34**, 4130 (2001).
21 S. L. Randzio, *Thermochim. Acta*, 2003, **398**, 75.
22 S. L. Randzio, *Thermochim. Acta*, 2000, **355**, 107.
23 S. L. Randzio, *J. Therm. Anal. Cal.*, 2007, **89**, 51.
24 M. Chorążewski, J-P.E. Grolier and S. L. Randzio, *J. Chem. Eng. Data*, 2010, **55**, 5489.
25 J. Troncoso, P. Navia, L. Romani, D. Bessieres and T. Lafitte, *J. Chem. Phys.*, 2011, **134**, 094502.
26 S. L. Randzio, J-P. E. Grolier, J. R. Quint, D. J. Eatough, E. A. Lewis and L. D. Hansen, *Int. J. Thermophys.*, 1994, **15**, 415.
27 M. Taravillo, V. G. Baonza, M. Caceres and J. Nunez, *J. Phys.: Condens. Matter*, 2003, **15**, 2979.
28 S. L. Randzio and U. K. Deiters, *Ber. Bunsenges. Phys. Chem.*, 1995, **99**, 1179.
29 U. K. Deiters and S. L. Randzio, *Fluid Phase Equilib.*, 1995, **103**, 199.
30 J. Troncoso, C. A. Cerdeiriña, P. Navia, Y. A. Sanmamed, D. González-Salgado and L. Romaní, *J. Chem. Phys. Lett.*, 2010, **1**, 211.
31 A. Grzybowski, M. Paluch and K. Grzybowska, *J. Phys. Chem. B*, 2009, **113**, 7419.
32 A. Grzybowski, M. Paluch and K. Grzybowska, *Phys. Rev. E*, 2010, **82**, 013501.
33 A. Grzybowski, S. Haracz, M. Paluch and K. Grzybowska, *J. Phys. Chem. B*, 2010, **114**, 11544.
34 A. Grzybowski, K. Grzybowska, M. Paluch, A. Swiety and K. Koperwas, *Phys. Rev. E*, 2011, **83**, 041505.
35 A. Grzybowski, K. Koperwas and M. Paluch, *Phys. Rev. E*, 2012, **86**, 031501.
36 A. Grzybowski, K. Koperwas and M. Paluch, *J. Chem. Phys.*, 2014, **140**, 044502.
37 G. Floudas, M. Paluch, A. Grzybowski and K. Ngai, *Molecular Dynamics of Glass-Forming Systems: Effects of Pressure*, Ch. 2, Series: *Advances in Dielectrics*, Series Editor: F. Kremer, Springer-Verlag: Berlin, Heidelberg, 2011
38 C. M. Roland, S. Hensel-Bielowka, M. Paluch and R. Casalini, *Rep. Prog. Phys.*, 2005, **68**, 1405.
39 C. M. Roland, S. Bair and R. Casalini, *J. Chem. Phys.*, 2006, **125**, 124508.
40 C. Alba-Simionesco and G. Tarjus, *J. Non-Cryst. Solids*, 2006, **352**, 4888.
41 U. R. Pedersen, N. P., Bailey, T. B., Schrøder and J. C. Dyre, *Phys. Rev. Lett.*, 2008, **100**, 015701.
42 N. P. Bailey, U. R., Pedersen, N. Gnan, T. B. Schrøder and J. C. Dyre, *J. Chem. Phys.*, 2008, **129**, 184507.
43 N. P. Bailey, U. R. Pedersen, N. Gnan, T. B. Schrøder and J. C. Dyre, *J. Chem. Phys.*, 2008, **129**, 184508.
44 D. Coslovich and C. M. Roland, *J. Phys. Chem. B*, 2008, **112**, 1329.
45 D. Coslovich and C. M. Roland, *J. Chem. Phys.*, 2009, **130**, 014508.
46 T. B. Schrøder, U. R. Pedersen, N. P. Bailey, S. Toxvaerd and J. C. Dyre, *Phys. Rev. E*, 2009, **80**, 041502.
47 A. Grzybowski, M. Paluch, K. Grzybowska and S. Haracz, *J. Chem. Phys.*, 2010, **133**, 161101.

48 M. Paluch, S. Haracz, A. Grzybowski, M. Mierzwa, J. Pionteck, A. Rivera-Calzada and C. Leon, *J. Phys. Chem. Lett.*, 2010, **1**, 987.

49 E. Masiewicz, A. Grzybowski, A. P. Sokolov and M. Paluch, *J. Phys. Chem. Lett.*, 2012, **3**, 2643.

50 Z. Wojnarowska, M., Paluch, A. Grzybowski, K., Adrjanowicz, K., Grzybowska, K., Kaminski, P. Wlodarczyk and J. Pionteck, *J. Chem. Phys.*, 2009, **131**, 104505.

51 K. Koperwas, A. Grzybowski, K. Grzybowska, Z. Wojnarowska, J. Pionteck, A. P. Sokolov and M. Paluch, *Phys. Rev. E*, 2012, **86**, 041502.

52 A. Grzybowski, K. Kolodziejczyk, K., Koperwas, K., Grzybowska and M. Paluch, *Phys. Rev. B*, 2012, **85**, 220201(R).

53 A. Swiety-Pospiech, Z. Wojnarowska, J. Pionteck, S. Pawlus, A. Grzybowski, S. Hensel-Bielowka, K. Grzybowska, A. Szulc and M. Paluch, *J. Chem. Phys.*, 2012, **136**, 224501.

54 E. R. López, A. S. Pensado, J. Fernández and K. R. Harris, *J. Chem. Phys.*, 2012, **136**, 214502.

55 A. Grzybowski, K. Koperwas, A. Swiety-Pospiech, K. Grzybowska and M. Paluch, *Phys. Rev. B*, 2013, **87**, 054105.

56 K. Adrjanowicz, A. Grzybowski, K. Grzybowska, J. Pionteck and M. Paluch, *Cryst. Growth Des.* 2014, **14**, 2097.

57 N. Gnan, T. B. Schrøder, U. R. Pedersen, N. P. Bailey and J. C. Dyre, *J. Chem. Phys.*, 2009, **131**, 234504.

58 T. B. Schrøder, N. Gnan, U. R. Pedersen, N. P. Bailey and J. C. Dyre, *J. Chem. Phys.*, 2011, **134**, 164505.

59 U. R. Pedersen, N. Gnan, N. P. Bailey, T. B. Schrøder and J. C. Dyre, *J. Non-Cryst. Solids*, 2011, **357**, 320.

60 T. S. Ingebrigtsen, L. Bøhling, T. B. Schrøder and J. C. Dyre, *J. Chem. Phys.*, 2012, **136**, 061102.

61 L. Bøhling, T. S. Ingebrigtsen, A. Grzybowski, M. Paluch, J. C. Dyre and T. B. Schrøder, *New J. Phys.*, 2012, **14**, 113035.

62 H. V. Kehiaian, J.-P. E. Grolier and G. C. Benson, *J. Chim. Phys.*, 1978, **75**, 1031.

63 H. V. Kehiaian, *Fluid Phase Equilib.*, 1983, **13**, 243.

64 O. Ciocirlan, M. Teodorescu, D. Dragoescu, O. Iulian, and A. Barhala, *J. Chem. Eng. Data*, 2010, **55**, 3891.

65 D. Gheorghe, D. Dragoescu, and M. Teodorescu, *J. Chem. Eng. Data*, 2013, **58**, 1161.

66 L. Fernández, D. Montaño, J. Ortega, and F.J. Toledo, *Ind. Eng. Chem. Res.*, 2013, **52**, 11758.

67 M. Artal, J. Muñoz-Embid, I. Velasco, S. Otin, *Phys. Chem. Liq.*, 2000, **38**, 537.

68 D. González-Salgado, J. Peleteiro, J. Troncoso, E. Carballo, and Luis Romani, *J. Chem. Eng. Data*, 2004,**49**,333.